Signal Flow Graph Block Approach to the Design of the Universal Mixed-mode Multi-loop Filter and Study of Non-ideal Properties

Roman Sotner, *Student member IEEE*, Josef Slezak, Tomas Dostal, and Jiri Frydrych

***Abstract*—The paper deals with the universal active filter design in current mode based on diamond transistors is presented. Circuit has abilities to work in high frequency range and adjustable features. All types of second order transfer functions are available. Theoretical assumptions are supported by simulation results in PSpice and by laboratory measurements. Impact of real substantial non-idealities caused by real active elements is discussed.**

***Index Terms*—Current-mode, voltage mode, universal filter, diamond transistors, adjustabilities, parasitic influences**

I. Introduction

IN the field of analog electronic circuit there are many suitable active elements for different applications in classical voltage mode (VM) and also in the new current mode (CM) [1], where much attention of the researchers is still focused. The actual state of the art of active elements for analog signal processing is very well described in [2]. We can mention for example the applications of the current conveyors (CC) [2-5], the current feedback amplifiers (CFA) [2, 6], the transconductors (OTA) [2, 7]. Novel modifications of the present and old active elements are for example the current follower transconductance amplifiers (CFTA) [8], the current conveyor transconductance amplifiers (CCTA) [9-11], the differential buffered transconductance amplifier (DBTA) [12] and others. These elements are suitable for design and applications of active filters, oscillators, modulators, mixers etc, working in the VM and especially in the CM. Advantages of these active blocks are small power consumption in CMOS technologies, high frequency bandwidth (i.e. GBW), easy implementation and possibilities of electronic adjusting, which is possible in most cases via biasing current or voltage. Actual trends are digital potentiometers, but due to the parasitic capacitances (tens pF) they are not suitable for high frequency applications. Most recent published works are focused on filters called Kerwin-Huelsman-Newcomb [13], which consist of two lossless integrators in two feedback loops. Another approach mentions lossless and lossy integrators in one loop feedback structure [14]. Majority of mentioned circuits provide basic transfer functions like high-pass (HP), band-pass (BP), low-pass (LP). Small modifications [15-17] allow extending to band-reject (BR) and all-pass (AP) filter responses. Many structures mentioned above use active elements with more current outputs that have been not commercially available yet. This is a disadvantage of the proposed solutions. The modern filter conceptions can be used in many applications such as anti-aliasing filter, in high-speed data telecommunication systems, for signal processing in cable modems, in regulation and measurement techniques etc. Diamond transistor (DT) is the commercially available active element (designate OPA 860 [18], together with high frequency voltage buffer) for high frequency purposes which can be described from two views (Fig. 1). The active elements in the mentioned solutions are based in most cases on the CMOS transistor structures, nevertheless the bipolar technology is more suitable for high frequency purposes, however power consumption is higher. The diamond transistor (DT) is commercially available active element, labeled OPA 860 [18] (together with high frequency voltage buffer). For high frequency purposes this element can be described from two views as shown in Fig. 1. The first one supposes that the DT is a OTA of the type SISO (single-input single-output) or of the type DISO (differential-input single-output), and the second view supposes that the DT is a current conveyor of the second generation (CCII).

Basic building blocks with the DT useable for proposed application are current integrator and current amplifier (Fig. 1).

R. Sotner is with the Brno University of Technology, Faculty of Electrical Engineering and Communication, Dept. of Radio electronics, Purkynova 118, Brno, 612 00, Czech Republic (e-mail: xsotne00@stud.feec.vutbr.cz).

J. Slezak is with the Brno University of Technology, Faculty of Electrical Engineering and Communication, Dept. of Radio electronics, Purkynova 118, Brno, 612 00, Czech Republic (e-mail: xsleza08@stud.feec.vutbr.cz).

T. Dostal is with the College of Polytechnics Jihlava, Tolsteho 16, Jihlava, 586 01, Czech Republic (e-mail: dostal@vspj.cz).

J. Frydrych is with the Brno University of Technology, Faculty of Electrical Engineering and Communication, Dept. of Radio electronics, Purkynova 118, Brno, 612 00, Czech Republic (e-mail: xfrydr02@stud.feec.vutbr.cz).

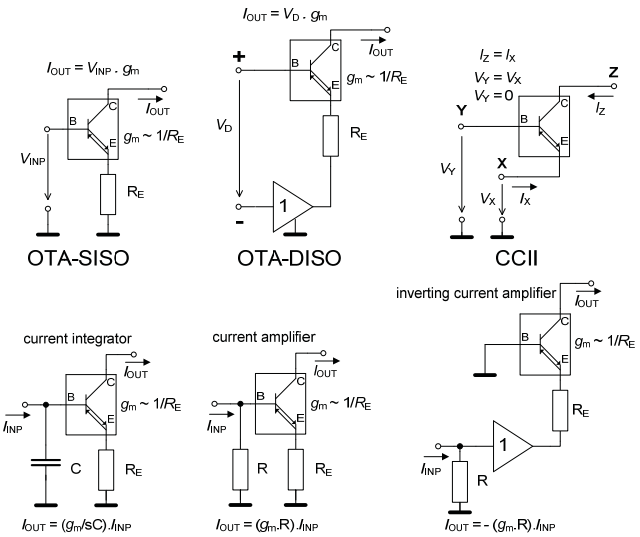

Fig. 1. Basic applications of the diamond transistor and elementary functional blocks suitable for next circuit design

II. Video Filter Based on Diamond Transistors

In Fig. 2 there is the signal flow graph which represents the basic current mode structure of the second order. The coefficients B are path transfers and f(s) are transfers of integrators. The graph contains two lossless integrators, two feedback branches, two summing nodes, one direct path and distribution point. This structure realizes three transfer functions namely low-pass (LP), band-pass (BP) and high-pass (HP). The corresponding circuit has only one distribution node. Modification for obtaining of the other types of the transfer characteristics is shown in Fig. 3. The graph includes second distribution node at the input and enables distributed input signal to all nodes designated as I_{INP_LP}, I_{INP_BP} and I_{INP_HP}. The modified structure (Fig. 3) can realize the following types: band-reject (BR), all-pass (AP) and LP or HP with zero. Simplest solution is using multi-output current follower (MO-CF) [19] in both distributed nodes [16, 17], but it has disadvantage, namely we can not adjust the gain in the separated braches or in the signal paths. However, this adjusting is necessary for to control of the quality factor (Q), the bandwidth (BW) of the BP, the basic gain (K_0) or location of the zero frequency (f_Z in HP, LP transfers with zeros). In this point of view the structure in Fig. 4 is more suitable. Here mentioned presumptions are fulfilled. The filter based on this structure is given in Fig. 5. Fundamental principle are described in the Fig. 2 and Fig. 3, but the input distributor is build as voltage to current converter and output voltage response is obtained on R_0. There for better impedance separation the output voltage follower is used.

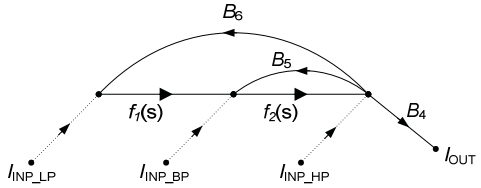

Fig. 2 Basic signal flow graph for distributed feedback current mode filter

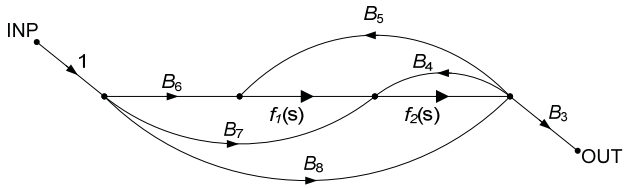

Fig. 4. Generalized signal flow graph of second order distributed feedback structure

Using the diamond transistors the parameters of the general graph (Fig. 4) are as follows and concrete graph is given in Fig. 5.

$$f_1(s) = \frac{g_{m1}}{sC_1},\ f_2(s) = \frac{g_{m2}}{sC_2}, \qquad (1), (2)$$

$$B_3 = -g_{m3}R_1,\ B_4 = -g_{m4}R_1,\ B_5 = g_{m5}R_1, \qquad (3), (4), (5)$$

$$B_6 = g_{m6},\ B_7 = g_{m7}, B_8 = g_{m8}, \qquad (6), (7), (8)$$

where g_{m6}, g_{m7}, g_{m8} (B_6, B_7, B_8 respectively) represents voltage to current conversion constants. The corresponding circuit in Fig. 5 includes switches for simple configuration of transfer functions. In Tab. 1 there are achievable transfer functions.

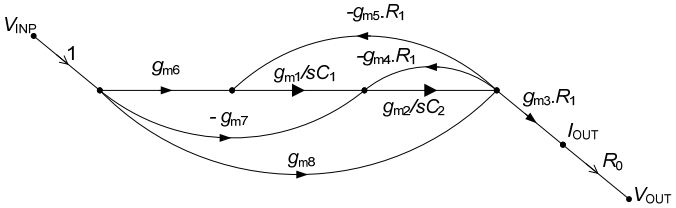

Fig. 4. Signal flow graph for concrete realization with DT-s

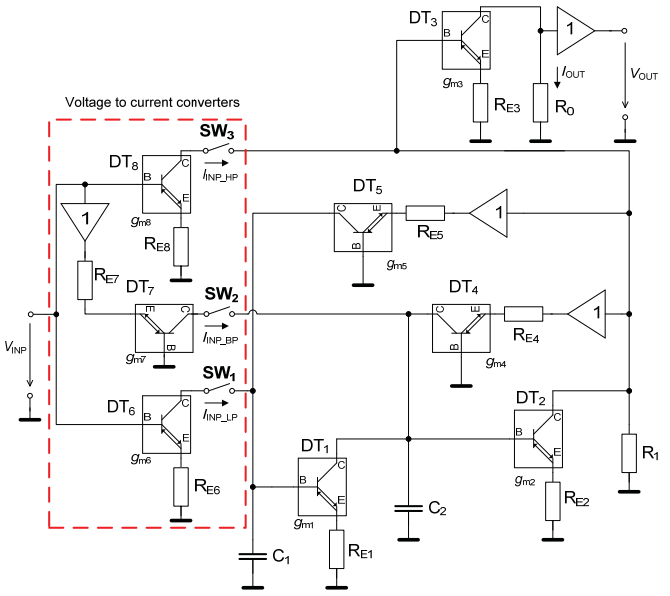

Fig. 5. Proposed universal filter with DT-s and buffers

TABLE I. Filter configurations

Transfer type	SW_1	SW_2	SW_3
Low-pass (LP)	on	off	off
Band-pass (BP)	off	on	off
High-pass (HP)	off	off	on
Band-reject (BR)	on	off	on
All-pass (AP)	on	on	on

The transfer functions and the characteristic frequency (f_C) and the quality factor (Q) have following forms

$$K_{LP}(s)=\frac{\frac{g_{m1}g_{m2}g_{m3}g_{m6}R_0R_1}{C_1C_2}}{s^2+\frac{g_{m2}g_{m4}R_1}{C_2}s+\frac{g_{m1}g_{m2}g_{m5}R_1}{C_1C_2}}, \quad (9)$$

$$K_{BP}(s)=\frac{-\frac{g_{m2}g_{m3}g_{m7}R_0R_1}{C_2}s}{s^2+\frac{g_{m2}g_{m4}R_1}{C_2}s+\frac{g_{m1}g_{m2}g_{m5}R_1}{C_1C_2}}, \quad (10)$$

$$K_{HP}(s)=\frac{g_{m3}g_{m8}R_0R_1s^2}{s^2+\frac{g_{m2}g_{m4}R_1}{C_2}s+\frac{g_{m1}g_{m2}g_{m5}R_1}{C_1C_2}}, \quad (11)$$

$$K_{BR}(s)=\frac{g_{m3}R_0R_1\left(g_{m8}s^2+\frac{g_{m1}g_{m2}g_{m6}}{C_1C_2}\right)}{s^2+\frac{g_{m2}g_{m4}R_1}{C_2}s+\frac{g_{m1}g_{m2}g_{m5}R_1}{C_1C_2}}, \quad (12)$$

$$K_{AP}(s)=\frac{g_{m3}R_0R_1\left(g_{m8}s^2-\frac{g_{m2}g_{m7}}{C_2}s+\frac{g_{m1}g_{m2}g_{m6}}{C_1C_2}\right)}{s^2+\frac{g_{m2}g_{m4}R_1}{C_2}s+\frac{g_{m1}g_{m2}g_{m5}R_1}{C_1C_2}}, \quad (13)$$

$$\omega_C=\sqrt{\frac{g_{m1}g_{m2}g_{m5}R_1}{C_1C_2}}, Q=\frac{C_2}{g_{m2}g_{m4}R_1}\sqrt{\frac{g_{m1}g_{m2}g_{m5}R_1}{C_1C_2}}. \quad (14), (15)$$

Sensitivities of the characteristic frequency and the quality factor on the circuit parameters are

$$S^{\omega_C}_{g_{m1}}=S^{\omega_C}_{g_{m2}}=S^{\omega_C}_{g_{m5}}=S^{\omega_C}_{R_1}=0.5, \quad (16)$$

$$S^{\omega_C}_{C_1}=S^{\omega_C}_{C_2}=-0.5, \quad (17)$$

$$S^{\omega_C}_{g_{m3}}=S^{\omega_C}_{g_{m4}}=S^{\omega_C}_{g_{m6}}=S^{\omega_C}_{R_7}=S^{\omega_C}_{R_8}=0, \quad (18)$$

$$S^{Q}_{g_{m1}}=S^{Q}_{g_{m5}}=S^{Q}_{C_2}=0.5, \quad (19)$$

$$S^{Q}_{g_{m2}}=S^{Q}_{R_1}=S^{Q}_{C_1}=-0.5, \quad (20)$$

$$S^{Q}_{g_{m4}}=-1, \quad S^{Q}_{g_{m3}}=S^{Q}_{g_{m6}}=S^{Q}_{g_{m7}}=S^{Q}_{g_{m8}}=0. \quad (21), (22)$$

III. Simulation Results

The filter in Fig. 5 was designed for the characteristic frequency f_C = 600 kHz and the quality Q = 1. Capacitors were chosen as $C_1 = C_2 = C$ = 470 pF. The transconductances were calculated accordingly to (14) and (15) as $g_{m1} = g_{m2}$ = 1.8 mS, $g_{m3} = g_{m4} = g_{m5}$ = 10 mS, $g_{m6} = g_{m7} = g_{m8}$ = 2.1 mS and R_1 = 100 Ω, R_0 = 470 Ω. Simulation results in PSpice are in Fig. 6 and Fig. 7. From simulation the value f_C = 588 kHz was obtained. Tuning of f_C for two values of capacitors is shown in Fig. 8 and Fig. 9. Adjusting of quality factor and BW of BP response is shown in Fig. 10 and adjusting of the gain of LP response is verified in Fig. 11.

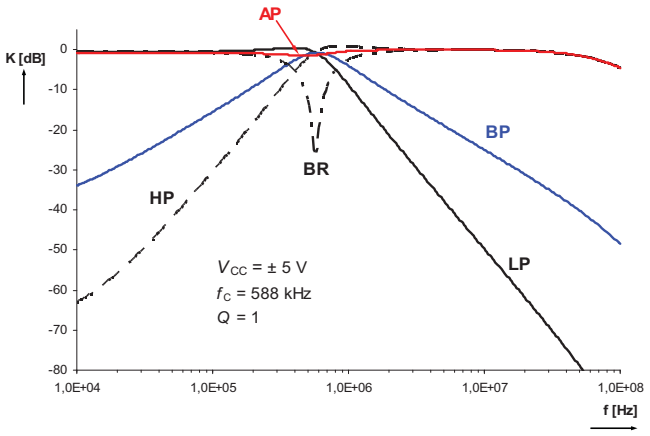

Fig. 6. Magnitude responses of proposed filter

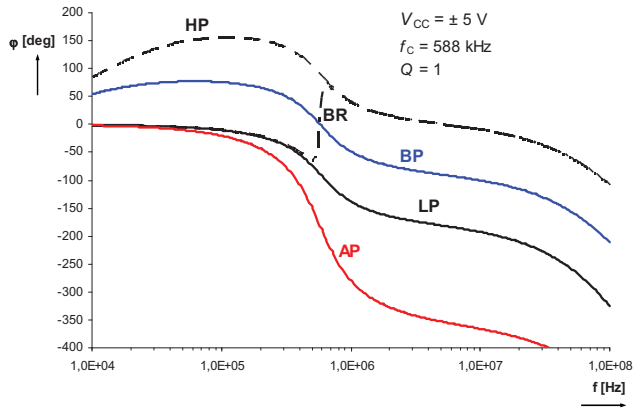

Fig. 7. Phase responses of proposed filter

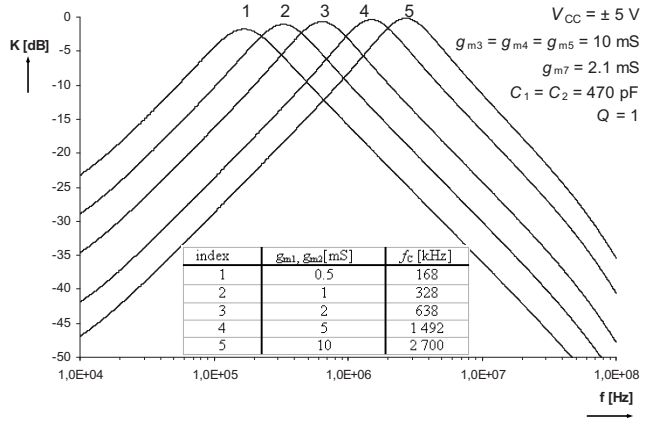

Fig. 8. Tunnig of the BP filter response via $g_{m1,2}$ (C = 470 pF)

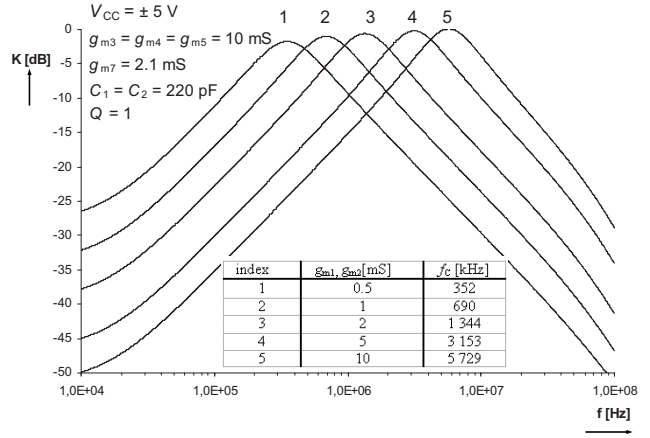

Fig. 9. Tunning of the BP filter response via $g_{m1,2}$ (C = 220 pF)

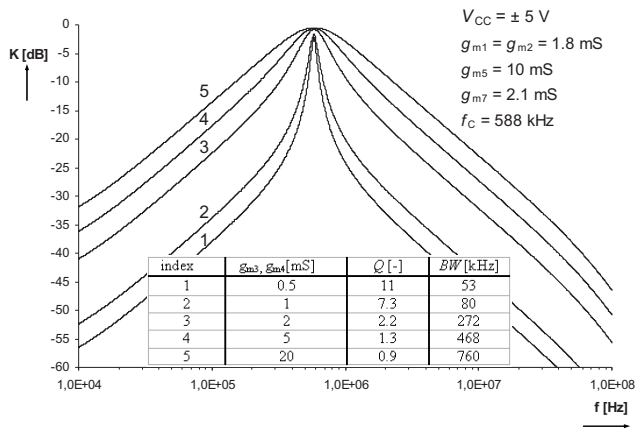

index	g_{m3}, g_{m4} [mS]	Q [-]	BW [kHz]
1	0.5	11	53
2	1	7.3	80
3	2	2.2	272
4	5	1.3	468
5	20	0.9	760

Fig. 10. Adjusting of Q and bandwidth on BP response

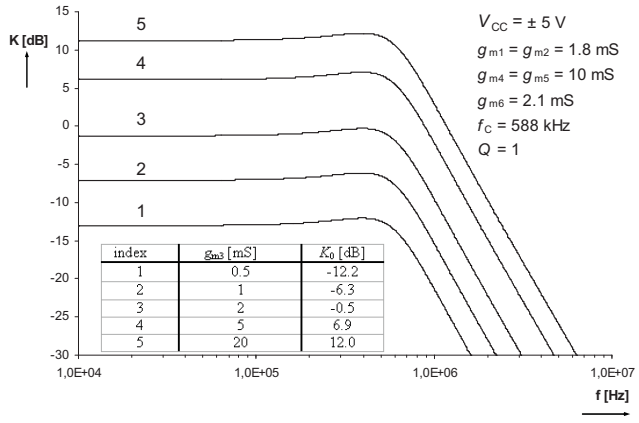

index	g_{m3} [mS]	K_0 [dB]
1	0.5	-12.2
2	1	-6.3
3	2	-0.5
4	5	6.9
5	20	12.0

Fig. 11. Adjusting of the gain (K_0) on LP response

IV. Experimental Results

The circuit in Fig. 5 was experimentally tested. Basic characteristic were measured. There was used network vector analyzer AGILENT E5071C. Results for design parameters mentioned in previous chapter are in Fig. 12 – Fig. 16. The value f_C = 560 kHz was obtained from measurements.

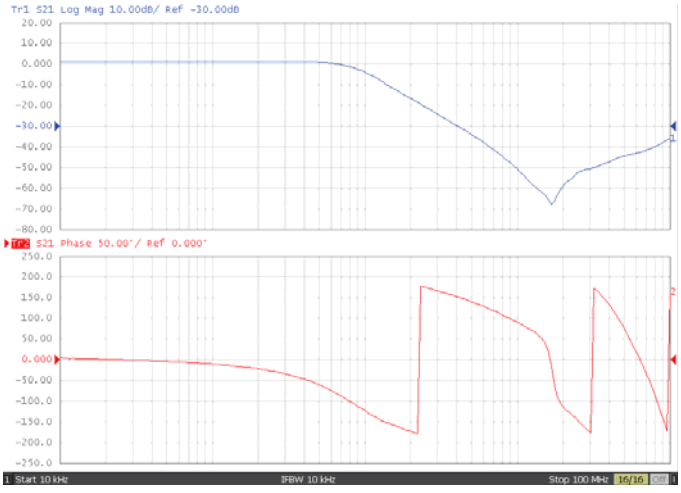

Fig. 12. Measured LP magnitude and phase response

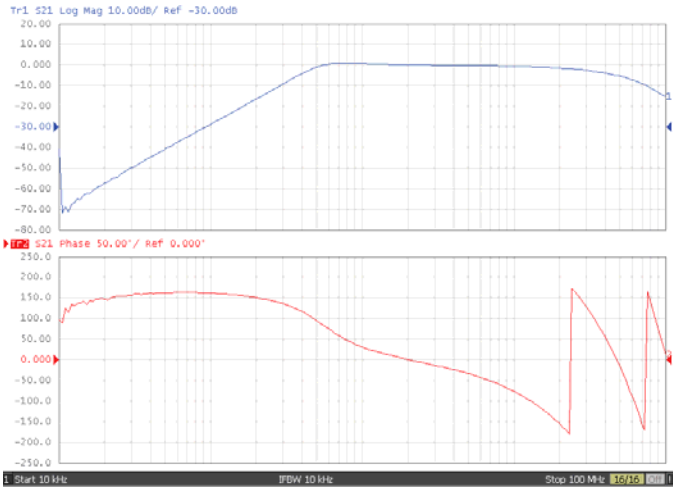

Fig. 13. Measured HP magnitude and phase response

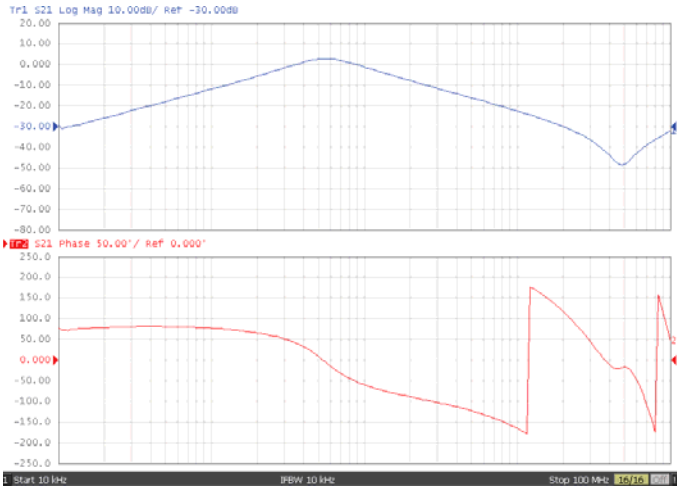

Fig. 14. Measured BP magnitude and phase response

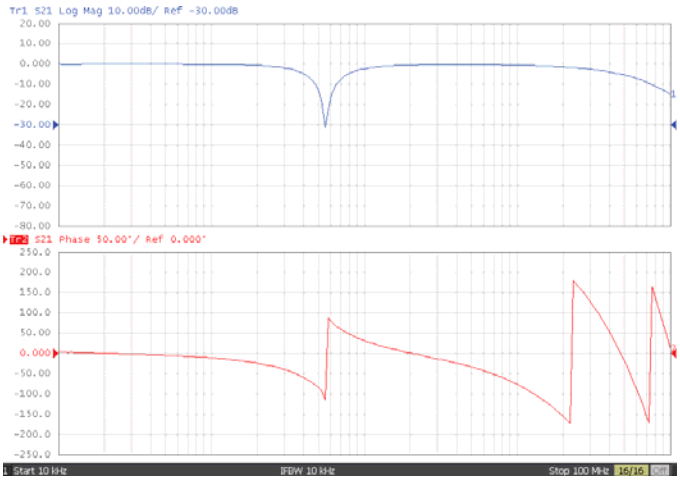

Fig. 15. Measured BR magnitude and phase response

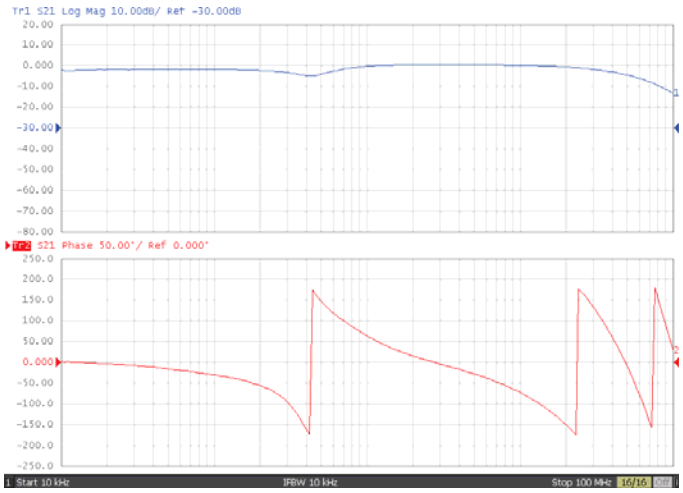

Fig. 16. Measured AP magnitude and phase response

V. Influences of Nonidealities of Real Active Elements

Real features of active elements play important role in behavior of designed application. In linear circuits and active filters there are some problems in stop band and pass band (parasitic zeros, finite attenuation in stop band). Of course, at higher frequencies finite frequency features of used active elements (gain) cause fall of voltage transfer in pass band in proposed applications. Node impedances in the circuit caused by real features of input and output of used active elements are responsible for some drawbacks in pass and stop band. In the current-mode or mixed mode circuits high impedances (high real part) in specific circuit nodes (outputs, capacitors in integrators) are important. Influences of these real parts are studied in detail in the following text. Also we can study complex problems (including parasitic capacitances) but mathematical description is too complicated and these capacitance causes only slight (several tens of kHz at video band) shift of characteristic frequency f_C (also causes fall of transfer characteristic at higher frequencies). Problems in stop band and pass band are caused by the real part of mentioned impedances. Therefore study of parasitic features was provided for resistances. The study is focused on three important nodes (Fig. 17).

In the proposed conception of filter DT and buffers are used (see the summary in Tab. 2.).

TABLE II. Input/Output Features of OPA 860

OPA 860				
DT				
R_c [kΩ]	R_b [kΩ]	R_e [Ω]	C_c [pF]	C_b [pF]
54	455	13	2	2.1
BUFFER				
R_{INP_BUFF} [MΩ]	R_{OUT_BUFF} [Ω]	C_{INP_BUFF} [pF]		
1	1.4	2.1		

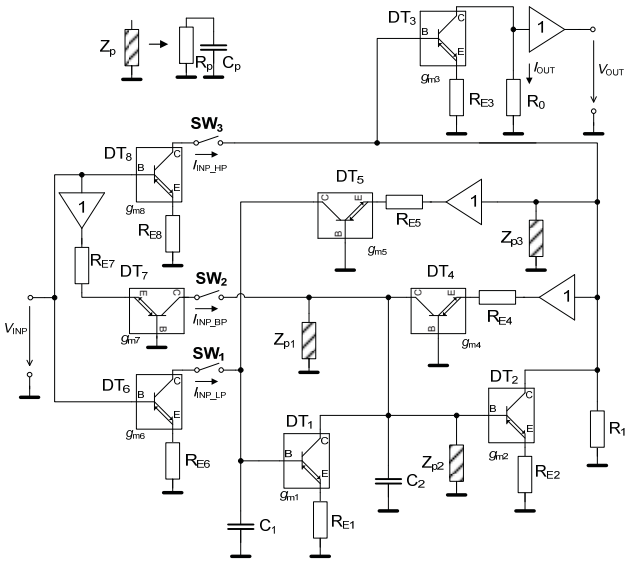

Fig. 17. Important parasitic influences in proposed filter structure

We can determine supposed values of parasitic elements

$$R_{p1} = \frac{1}{\frac{1}{R_{c\_DT6}} + \frac{1}{R_{c\_DT5}} + \frac{1}{R_{b\_DT1}}} = 25.5\ k\Omega\,, \tag{23}$$

$$R_{p2} = \frac{1}{\frac{1}{R_{c\_DT7}} + \frac{1}{R_{c\_DT4}} + \frac{1}{R_{c\_DT1}} + \frac{1}{R_{b\_DT2}}} = 17.3\ k\Omega\,, \tag{24}$$

$$R_{p3} = \frac{1}{\frac{1}{R_{c\_DT8}} + \frac{1}{R_{c\_DT2}} + \frac{1}{R_{INP\_BUFF1}} + \frac{1}{R_{INP\_BUFF1}}} = 25.6\ k\Omega\,. \tag{25}$$

Further analysis will show sufficiency of these values. After that the filter transfer functions contain additional elements that are defined by equations (23-25). Denominator of the transfer function is

$$D^*(s) = b_2^* s^2 + b_1^* s + b_0^*, \tag{26}$$

where coefficients are

$$b_2^* = 1, \tag{27}$$

$$b_1^* = \frac{g_{m2}g_{m4}R_1R_{p1}R_{p2}R_{p3}C_1 + (R_1 + R_{p3})(R_{p1}C_1 + R_{p2}C_2)}{C_1C_2R_{p1}R_{p2}(R_1 + R_{p3})}, \tag{28}$$

$$b_0^* = \frac{g_{m2}R_1R_{p2}R_{p3}(g_{m1}g_{m5}R_{p1} + g_{m4}) + R_1 + R_{p3}}{C_1C_2R_{p1}R_{p2}(R_1 + R_{p3})}\,. \tag{29}$$

Band pass filter transfer function has following form

$$K_{BP}^*(s) = \frac{\frac{-g_{m2}g_{m3}g_{m7}R_0R_1R_{p2}R_{p3}(sC_1R_{p1} + 1)}{C_1C_2R_{p1}R_{p2}(R_1 + R_{p3})}s}{D^*(s)}\,. \tag{30}$$

One parasitic zero is given by

$$z_1 = -\frac{1}{R_{p1}C_1}. \tag{31}$$

The limit case at low frequencies (several kHz) the stop band transfer function is given by form

$$K^*_{BP}(\omega \to 0) = \lim_{\omega \to 0} K^*_{BP} = \\ = \frac{g_{m2}g_{m3}g_{m7}R_0R_1R_{p2}R_{p3}}{g_{m2}R_1R_{p2}R_{p3}\left(g_{m1}g_{m5}R_{p1}+g_{m4}\right)+R_1+R_{p3}}, \tag{32}$$

for assumed values from section III and values of the parasitic resistances evaluated above the limit transfer is $|K_{BP}^*(0)|$ = -33.5 dB. This problem is more obvious from Fig. 18.

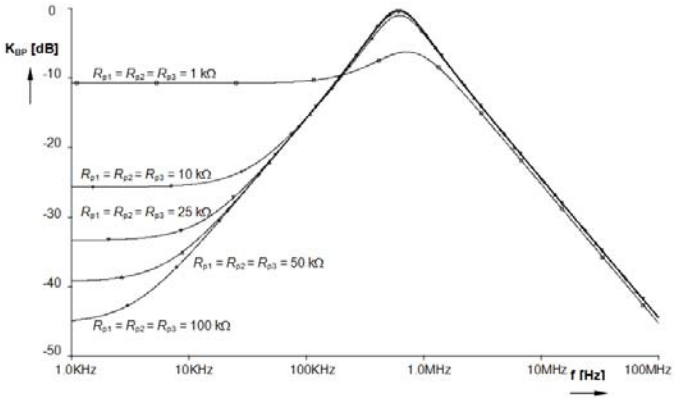

Fig. 18. Influence of simultaneous changes of R_{p1}, R_{p2} and R_{p3} on BP magnitude response

The characteristics in Fig. 19 - 21 show impact of all resistances R_{p1}-R_{p3} separately thus we can determine how each parasitic element affects behavior of BP filter response.

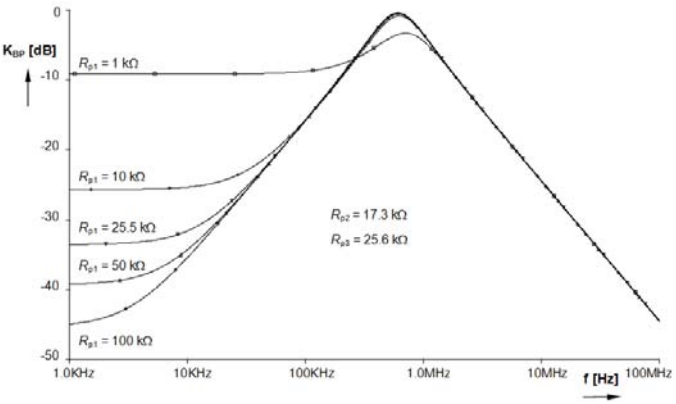

Fig. 19. Influence of separated R_{p1} (R_{p2} and R_{p3} are constant) changes on BP

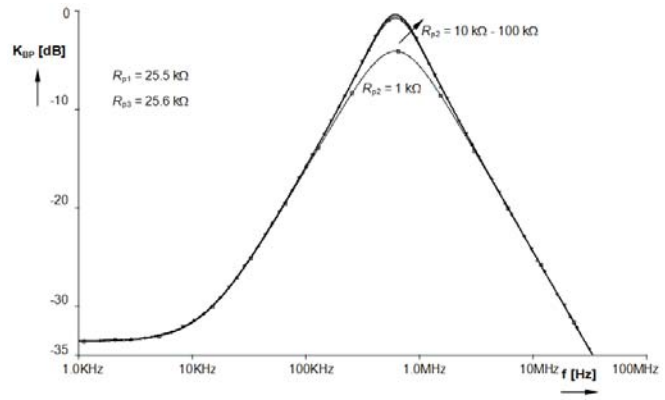

Fig. 20. Influence of separated R_{p2} (R_{p1} and R_{p3} are constant) changes on BP

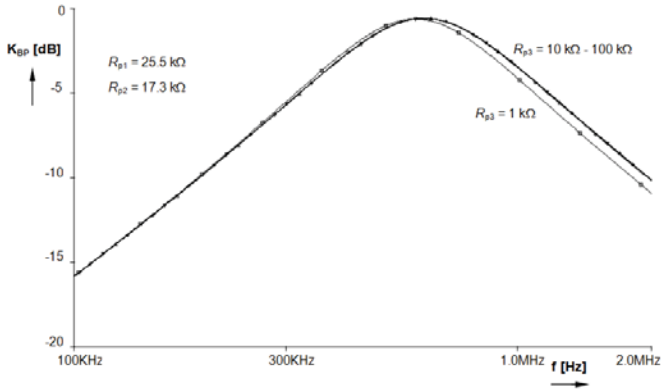

Fig. 21. Influence of separated R_{p3} (R_{p1} and R_{p2} are constant) changes on BP

From previous results we can determine following conclusions. R_{p1} has the main impact on stop band attenuation of BP, R_{p2} affects pass band transfer (Fig. 20) and R_{p3} causes slight shift of f_C (mainly for small values of R_{p3}). It`s clear from the results that recommend values for R_p are more than 100 kΩ (mainly for R_{p1}). Unfortunately in design of active elements and their features there are very often contradictory requirements on bandwidth and small signal parameters. Therefore it is always a compromise.

Similarly following transfer function which includes parasitic components was determined for HP

$$K^*_{HP}(s) = \frac{a_2^* s^2 + a_1^* s + a_0^*}{D^*(s)}, \tag{33}$$

$$a_2^* = \frac{g_{m3}g_{m7}R_0R_1R_{p3}}{R_1+R_{p3}}, \tag{34}$$

$$a_1^* = \frac{g_{m3}g_{m7}R_0R_1R_{p3}\left(C_1R_{p1}+C_2R_{p2}\right)}{C_1C_2R_{p1}R_{p2}\left(R_1+R_{p3}\right)}, \tag{35}$$

$$a_0^* = \frac{g_{m3}g_{m7}R_0R_1R_{p3}}{C_1C_2R_{p1}R_{p2}\left(R_1+R_{p3}\right)}. \tag{36}$$

Zeros are

$$z_1 = -\frac{1}{R_{p1}C_1},\ z_2 = -\frac{1}{R_{p2}C_2}. \tag{37}$$

Transfer at low frequencies is given by

$$K_{HP}^{*}(\omega \to 0) = \lim_{\omega \to 0} K_{HP}^{*} = \\ = \frac{g_{m3} g_{m7} R_0 R_1 R_{p3}}{g_{m2} R_1 R_{p2} R_{p3} \left(g_{m1} g_{m5} R_{p1} + g_{m4} \right) + R_1 + R_{p3}} , \quad (38)$$

where numerical value of transfer is $|K_{HP}^{*}(0)|$ = - 63.4 dB. Graphical representation is in Fig. 22 - 25.

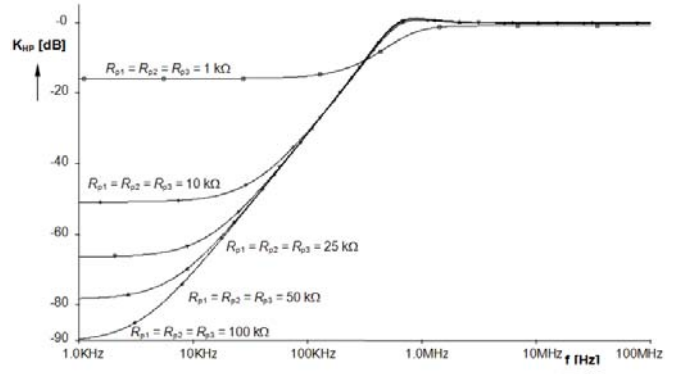

Fig. 22. Influence of simultaneous changes of R_{p1}, R_{p2} and R_{p3} on HP magnitude response

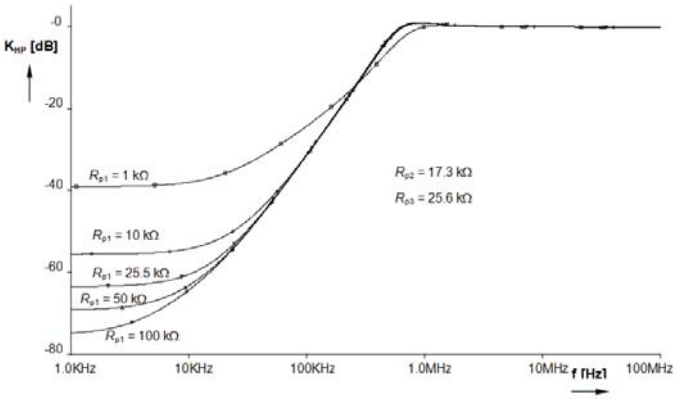

Fig. 23. Influence of separated R_{p1} (R_{p2} and R_{p3} are constant) changes on HP

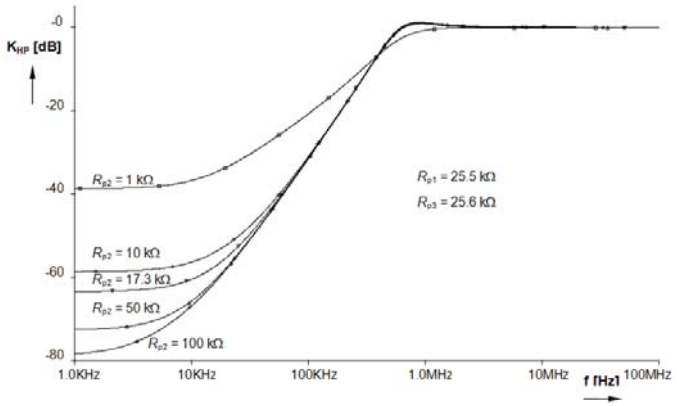

Fig. 24. Influence of separated R_{p2} (R_{p1} and R_{p3} are constant) changes on HP

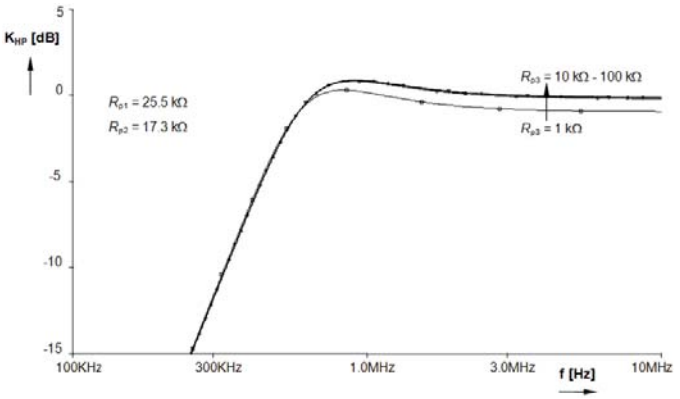

Fig. 25. Influence of separated R_{p3} (R_{p1} and R_{p2} are constant) changes on HP

It`s clear from previous results that values of R_p larger than several tens of kΩ are sufficient for good attenuation is stop band. Influence of values of R_{p1} and R_{p2} on stop band is similar, R_{p3} influences mainly pass band transfer of HP response.

For BR response, similar equations like in previous case is valid

$$K_{BR}^{*}(s) = \frac{a_2^{*} s^2 + a_1^{*} s + a_0^{*}}{D^{*}(s)} , \quad (39)$$

where both first coefficients a_2^{*} and a_1^{*} are very similar but a_0^{*} is different

$$a_2^{*} = \frac{g_{m3} g_{m8} R_0 R_1 R_{p3}}{R_1 + R_{p3}} , \quad (40)$$

$$a_1^{*} = \frac{g_{m3} g_{m8} R_0 R_1 R_{p3} \left(C_1 R_{p1} + C_2 R_{p2} \right)}{C_1 C_2 R_{p1} R_{p2} \left(R_1 + R_{p3} \right)} , \quad (41)$$

$$a_0^{*} = \frac{g_{m3} R_0 R_1 R_{p3} \left(g_{m1} g_{m2} g_{m6} R_{p1} R_{p2} + g_{m8} \right)}{C_1 C_2 R_{p1} R_{p2} \left(R_1 + R_{p3} \right)} . \quad (42)$$

Transfers at low and high frequencies in pass band of BR magnitude characteristic are given by

$$K_{BR}^{*}(\omega \to \infty) = \lim_{\omega \to \infty} K_{BR}^{*} = \frac{g_{m3} g_{m8} R_0 R_1 R_{p3}}{R_1 + R_{p3}} , \quad (43)$$

$$K_{BR}^{*}(\omega \to 0) = \lim_{\omega \to 0} K_{BR}^{*} = \\ = \frac{g_{m3} R_0 \left(g_{m1} g_{m2} g_{m6} R_{p1} R_{p2} + g_{m8} \right)}{g_{m2} R_{p2} \left(g_{m1} g_{m5} R_{p1} + g_{m4} \right) + R_1 + R_{p3}} , \quad (44)$$

After substitution of the numerical values in the symbolical equations the corresponding results show that transfers are slightly affected, $|K_{BR}^{*}(0)|$ = - 0.3 dB and $|K_{BR}^{*}(\infty)|$ = - 0.15 dB. For values taken from chapter III and parasitic resistances estimated using (23-25) the minimum of transfer function at f_C (stop band of BR) is $|K_{MIN}|$ = - 25.5 dB. The associated results are provided in Fig. 26 - 39.

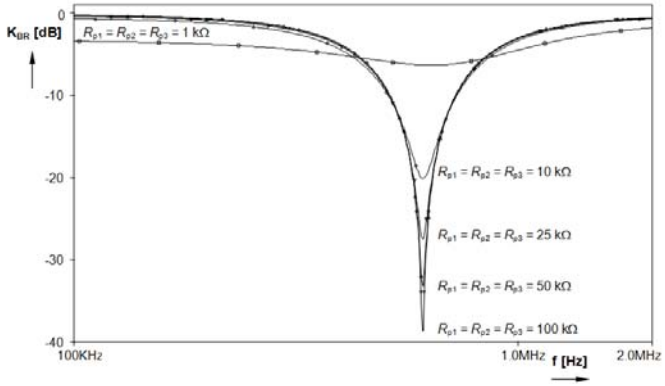

Fig. 26. Influence of simultaneous changes of R_{p1}, R_{p2} and R_{p3} on BR magnitude response

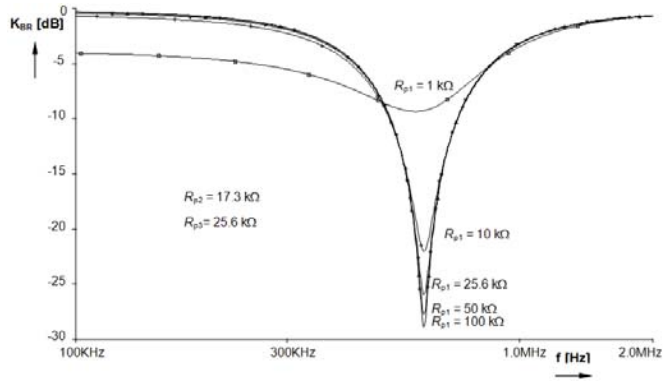

Fig. 27. Influence of separated R_{p1} (R_{p2} and R_{p3} are constant) changes on BR

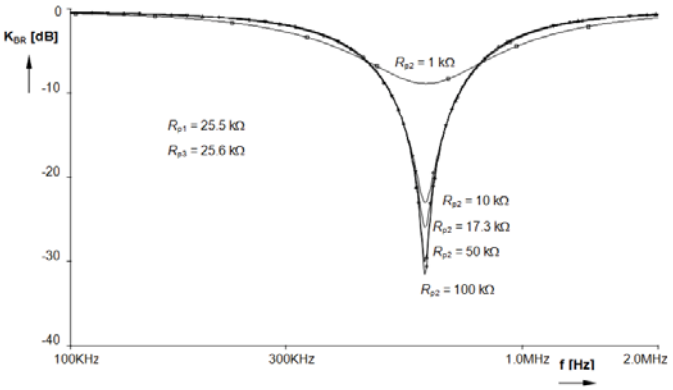

Fig. 28. Influence of separated R_{p2} (R_{p1} and R_{p3} are constant) changes on BR

Resistance R_{p1} causes problems in pass band at low frequencies and also contributes to decrease of attenuation in stop band. Similar effect has R_{p2} however this parameter influences only maximal stop band attenuation (Fig. 28). Parasitic element R_{p3} decreases pass band transfer at higher frequencies but only for values of several units of kΩ. For maximal attenuation in stop band of BR values of R_p of 100 kΩ and higher are necessary.

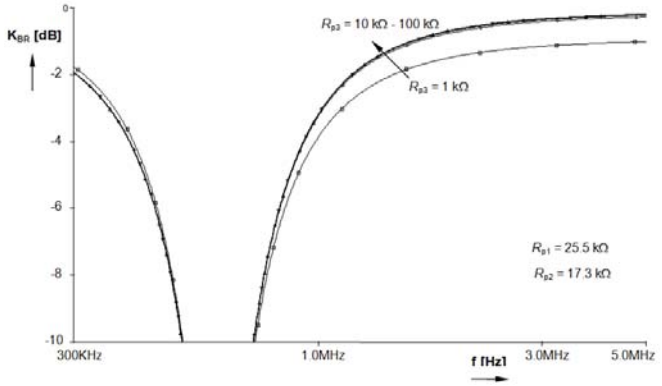

Fig. 29. Influence of separated R_{p3} (R_{p1} and R_{p2} are constant) changes on BR

The same analysis was provided for all pass filter. Transfer function affected by parasitic nodes resistances has form

$$K_{AP}^*(s) = \frac{a_2^* s^2 - a_1^* s + a_0^*}{D^*(s)}, \tag{45}$$

where coefficients are

$$a_2^* = \frac{g_{m3} g_{m8} R_0 R_1 R_{p3}}{R_1 + R_{p3}}, \tag{46}$$

$$a_1^* = \frac{g_{m3} R_0 R_1 R_{p3} \left[g_{m8} \left(C_1 R_{p1} - C_2 R_{p2} \right) + g_{m2} g_{m7} C_1 R_{p1} R_{p2} \right]}{C_1 C_2 R_{p1} R_{p2} (R_1 + R_{p3})}, \tag{47}$$

$$a_0^* = \frac{g_{m3} R_0 R_1 R_{p3} \left(g_{m1} g_{m2} g_{m6} R_{p1} R_{p2} + g_{m8} - g_{m2} g_{m7} R_{p2} \right)}{C_1 C_2 R_{p1} R_{p2} (R_1 + R_{p3})}. \tag{48}$$

Again, transfer characteristic has slight decreases in low and high frequency bands which is caused by parasitic elements.

$$K_{AP}^*(\omega \to \infty) = \lim_{\omega \to \infty} K_{AP}^* = \frac{g_{m3} g_{m8} R_0 R_1 R_{p3}}{R_1 + R_{p3}}, \tag{49}$$

$$K_{AP}^*(\omega \to 0) = \lim_{\omega \to 0} K_{AP}^* = \\ = \frac{g_{m3} R_0 R_1 R_{p3} \left(g_{m1} g_{m2} g_{m6} R_{p1} R_{p2} + g_{m8} - g_{m2} g_{m7} R_{p2} \right)}{g_{m2} R_1 R_{p2} R_{p3} \left(g_{m1} g_{m5} R_{p1} + g_{m4} \right) + R_1 + R_{p3}}. \tag{50}$$

Numerical values are $|K_{AP}^*(0)|$ = - 0.5 dB and $|K_{AP}^*(\infty)|$ = - 0.15 dB. Corresponding results are in Fig. 30 - Fig. 33.

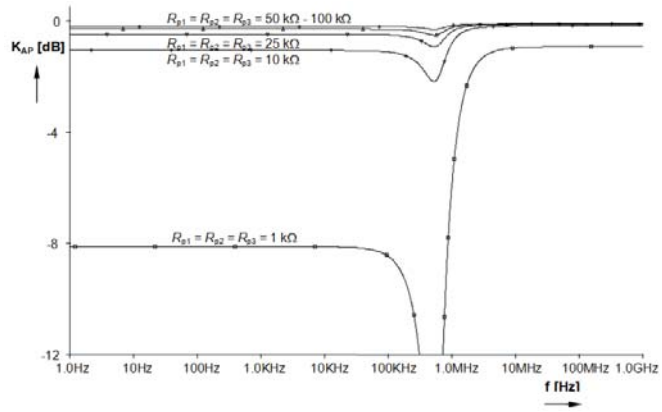

Fig. 30. Influence of simultaneous changes of R_{p1}, R_{p2} and R_{p3} on AP magnitude response

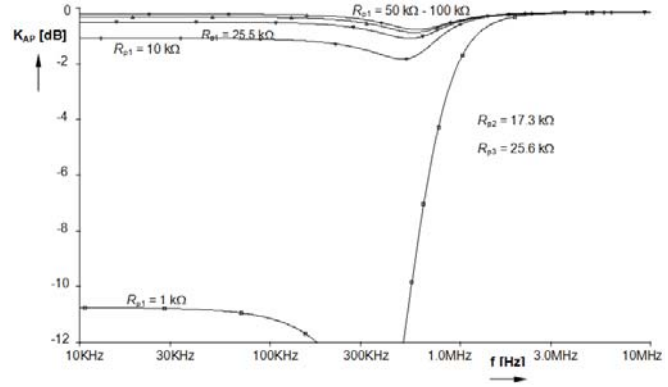

Fig. 31. Influence of separated R_{p1} (R_{p2} and R_{p3} are constant) changes on AP

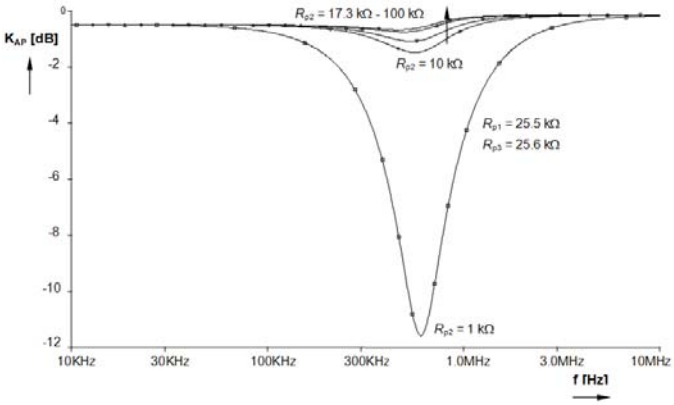

Fig. 32. Influence of separated R_{p2} (R_{p1} and R_{p3} are constant) changes on AP

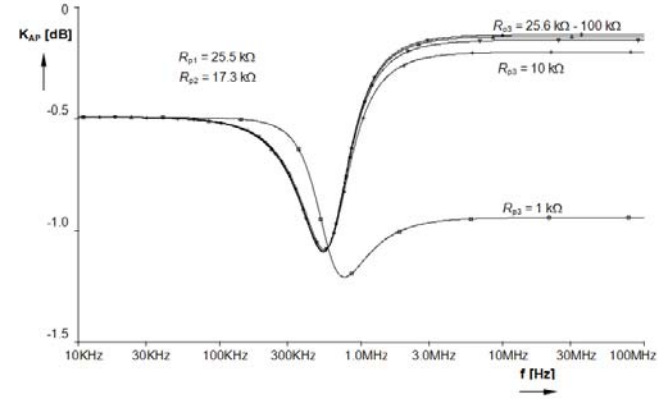

Fig. 33. Influence of separated R_{p3} (R_{p1} and R_{p2} are constant) changes on AP

Main impact on AP response is at low frequencies where R_{p1} is very important. The influence of R_{p1} is evident if its values are smaller than 50 kΩ (Fig. 31). Parameter R_{p2} affects AP response at f_C and neighborhood of f_C (Fig. 32). R_{p3} causes small decrease of AP transfer at high frequencies (Fig. 33).

The mentioned parasitic problems negligibly affects the low pass response. Transfer function contains parasitic elements but there are not problems with finite stop band attenuation or parasitic zeros

$$K_{LP}^{*}(s)=\frac{\dfrac{g_{m1}g_{m2}g_{m3}g_{m7}R_0R_1R_{p3}}{C_1C_2\left(R_1+R_{p3}\right)}}{D^{*}(s)}. \qquad (51)$$

In fact parasitic influences are very important for analog circuit design. There were discussed mainly parameters affecting transfer function features. For example accuracy of characteristic frequency f_C was not discussed. It depends also on parasitic capacitances, frequency features of used active elements (gain), and also on resistances of R_e (internal emitor resistance of current input) of used diamond transistors (DT). This is caused by $R_{E1} = 1/g_{m1} + R_{e1}$ and similarly for next R_E connected in emitors of DTs. It is necessary to take it into account.

From the text above it is clear that analysis of the parasitic behavior are very complex and difficult task.

VI. Conclusion

A signal flown graph technique was used to synthesize universal active filter using diamond transistor. The circuit has capabilities of electronic adjusting of many important parameters like characteristic frequency, quality factor, bandwidth of BP and the gain. Active and passive sensitivities are low. The circuit was tested by simulation and measurement in video band. Experimental results are in good agreement to the theory and simulations. Advantage of this conception is in possibilities of obtaining of HP and LP response with zero and in adjusting of f_Z. Detailed study of influences of parasitic elements was provided for nodal resistances in circuit structure. Digital control of analog circuits is important part of present development. Novel approaches (similar like in this paper) based on modern active elements allow simpler implementation of digital driving [21] than common operational amplifiers.

Acknowledgment

Research described in the paper was supported by the Czech Ministry of Education under research program MSM 0021630513 and Czech Science Foundation projects under No. 102/08/H027 and No. 102/09/1681. Research described in the paper is a part of the COST Action IC0803 RF/Microwave communication subsystems for emerging wireless technologies, financed by the Czech Ministry of Education by the grant no. OC09016.

References

[1] C. Toumazou, F. J. Lidgey, D. G. Haigh, "Analogue IC design: The current mode approach," Peter Peregrinus Ltd., London, 1990

[2] D. Biolek, R. Senani, V. Biolkova, Z. Kolka, "Active elements for analog signal processing: Classification, Review and New Proposal," *Radioengineering*, vol. 17, no. 4, pp. 15-32, 2008.

[3] D. Biolek, K. Vrba, J. Cajka, T. Dostal, "General three-port current: a useful tool for network design," *Journal of Electrical Engineering*, vol. 51, no. 1-2, pp. 36-39, 2000.

[4] J. Jerabek, K. Vrba, "Novel Universal Filter Using Only two Current Active Elements," *Proceedings of the Third International Conference on Systems ICONS08*, Cancun, Mexico, IEEE Computer Society, pp. 285-289, 2008.

[5] C. Wang, Y. Zhao, Q. Zhang, S. Du, "A new current mode SIMO-type universal biquad employing multi-output current conveyors (MOCCIIs)," *Radioengineering*, vol. 18, no. 1, p. 83 – 88, 2008.

[6] M. Siripruchyanun, C. Chanapromma, P. Silapan, W. Jaikla, " BiCMOS Current-Controlled Current Feedback Amplifier (CC-CFA) and Its Applications," *WSEAS Transactions on Electronics*, vol. 5, no. 6, pp. 203-219, 2008.

[7] D. Biolek, V. Biolkova, Z. Kolka, "Universal current-mode OTA-C KHN biquad," *International Journal of Electronics*, vol. 1, no. 4, pp. 214-217, 2007.

[8] N. Herencsar, J. Koton, K. Vrba, J. Misurec, "A novel Current-Mode SIMO Type Universal Filter Using CFTAs," *Contemporary Engineering Sciences*, vol. 2, no. 2, pp. 59-66, 2009.

[9] R. Prokop, V. Musil, "CCTA a new modern circuit block and its internal realization," *Electronic Devices and Systems IMAPS CZ International Conference Brno*, Czech Republic, pp. 89-93, 2005.

[10] R. Prokop, V. Musil, "New modern circuit block CCTA and some its applications," *The Fourteenth International Scientific and Applied Science Conference Electronics ET'2005*, Book 5. Sofia, TU-Sofia, pp. 93-98, 2005.

[11] R. Prokop, V. Musil, "Modular approach to design of modern circuit blocks for current signal processing and new device CCTA," *Proceedings of the Seventh IASTED International Conference on Signal and Image Processing*. Anaheim, USA, ACTA Press, pp. 494-499, 2005.

[12] N. Herencsar, K. Vrba, J. Koton, I. Lattenberg , "The conception of differential-input buffered and transconductance amplifier (DBTA) and its application," *IEICE Electronics Express*, vol. 6, no. 6, pp. 329-334, 2009.

[13] W. J. Kerwin, L. P. Huelsman, W. R. Newcomb, "State variable synthesis for insensitive integrated circuit transfer functions," *IEEE-SC*, vol. 2, no. 2, pp. 87-92, 1967.

[14] T. Tsukutani, Y. Sumi, Y. Fukui, "Electronically tunable current-mode OTA-C biquad using two-integrator loop structure," *Frequenz*, vol. 60, no. 3-4, pp. 53-56, 2006.

[15] R. Sotner, J. Petrzela, J. Slezak, "Current-Controlled Current-Mode Universal Biquad Employing Multi-Output Transconductors," *Radioengineering,* vol. 18, no. 3, pp. 285-294, 2009.

[16] T. Dostal, "Filters with multi-loop feedback structure in current mode," *Radioengineering*, vol. 12, no. 3, pp. 6-11, 2003.

[17] R. Sotner, J. Slezak, T. Dostal, J. Petrzela, "Universal tunable current-mode biquad employing distributed feedback structure with MO-CCCII," *Journal of Electrical Engineering*, vol. 61, no. 1, pp. 52-56, 2010.

[18] Texas Instruments Inc. OPA 860 Wide Bandwidth Operational Transconductance Amplifier and Buffer. 2006, datasheet, 32 p. accessible on www: http://www.ti.com

[19] J. Jerabek, K. Vrba, "Multiple-input Multiple-output Univresal Filter Using Current Followers," *Proceedings of the 31t International Conference on Telecommunications and Signal Processing – TSP 2008*, Budapest, Hungary, pp. 29-32, 2008.

[20] Intersil. Current-mode four-quadrant multiplier EL 4083. 1993, datasheet, 16 p., accessible on http://www.elantec.com

[21] B. Sevcik, "Modelling and Signal Integrity Testing of Digital Potentiometers," *Proceedings of the 17th International Conference Mixed Design of Integrated Circuits and System MIXDES 2010*, Wroclav, Poland, pp. 570-575, 2010.

Roman Sotner was born in Znojmo, Czech Republic, in 1983. He received the MSc. degree (2008) from the Brno University of Technology. Currently he is Ph.D. student at the Faculty of Electrical Engineering and Communication. His interests are analog circuits (active filters, oscillators, audio, etc.), circuits in the current mode and computer simulation. He is author and coauthor of several papers at conference proceedings and in international journals. He is student member IEEE.

Josef Slezak was born in Zlin, Czech Republic, in 1982. He received his MSc. degree in 2007 from the University of Technology, Brno. He is currently studying his Ph.D. study at the same university. His research interest is in analysis and design of analog circuits and computer optimalization methods. He is author and coauthor of several papers in international journals and conference proceedings.

Tomas Dostal (*1943) received his Ph.D. (1976) and Dr.Sc. degree (1989). He was with the University of Defense Brno (1976-1978 and 1980-1984), with the Military Technical College Baghdad (1978-1980), with the Brno University of Technology (1984-2008) and with the European Polytechnic Institute (2008 - 2009). Since 2009 he has been with the College of Polytechnics, Jihlava as Professor of Electronics. His interests are in circuit theory, analog filters, switched capacitor networks and circuits in the current mode.

Jiri Frydrych was born in Vsetin, Czech Republic, in 1986. He received his MSc. degree in 2010 from the University of Technology, Brno. He is currently studying his Ph.D. study at the Faculty of Electrical Engineering and Communication. He interest in analogue circuits, modern active functional blocks, design of analog circuits operating in current mode and various circuits with microprocessors and microwave techniques.